Nucleation and growth of Si(111)-$\sqrt{3}\times\sqrt{3}$-Ag investigated *in situ* using second-harmonic generation

Dongmei Deng[1,2] and Takanori Suzuki[1,*]

[1]*Riken, The Institute of Physical and Chemical Research, Hirosawa 2-1, Wako, Saitama 351 0198, Japan*
[2]*Graduate School of Science and Engineering, Saitama University, Shimo-Okubo 255, Sakura-ku, Saitama 338-8570, Japan*

Second-harmonic generation (SHG) has been used to monitor the adsorption of Ag on the Si(111)-7×7 surface and its successive transformation to Si(111)-$\sqrt{3}\times\sqrt{3}$-Ag *in situ* at several sample temperatures in the range from 190 °C to 570 °C. The decrease of the SH intensity with Ag deposition at elevated temperatures higher than about 200 °C was found to be a result of destructive interference between the SH signals from Si(111)-7×7 and Si(111)-$\sqrt{3}\times\sqrt{3}$-Ag. The temporal dependence of the SH intensity was calculated for a direct transformation model of Si(111)-$\sqrt{3}\times\sqrt{3}$-Ag formation. The calculation using the phase differences and the desorption rates obtained from the SH signal shows a temperature-dependent systematic deviation from the observed data; that is, reduced transformation to Si(111)-$\sqrt{3}\times\sqrt{3}$-Ag in the initial stage of Ag deposition as compared with that in the direct transformation model, which clearly suggests the existence of a critical size of Ag islands for the nucleation of Si(111)-$\sqrt{3}\times\sqrt{3}$-Ag. Once nucleated, the Si(111)-$\sqrt{3}\times\sqrt{3}$-Ag transformation is indicated to be accelerated by the additionally deposited Ag atoms up to a Ag coverage, at which point all the deposited Ag atoms are incorporated into the reconstruction. Moreover, the peak of a polarization-selected SHG signal observed during desorption was found to correspond to a surface fully covered by the 3×1 structure with a Ag coverage of 1/3 monolayer.

I. INTRODUCTION

Studies of a few monolayers of Ag on Si(111) have been conducted intensively because of the scientific and technological interests.[1] It is established that at room temperature, the Ag layer grows in a quasi-Frank-van der Merwe mode up to a few monolayers (MLs). A two-dimensional wetting layer, which was observed to consist of a network of Ag clusters with a complex structure in half-unit cells of Si(111)-7×7 (hereafter referred to as 7×7) reconstruction,[2] grows from the beginning of Ag deposition, followed by the growth of three-dimensional (3D) islands after the completion of the growth of the Ag wetting layer.[3–9] Above the phase transformation temperature T_c (about 200 °C), Ag grows in the Stranski-Krastanov mode; a Si(111)-$\sqrt{3}\times\sqrt{3}$-Ag (hereafter referred to as $\sqrt{3}\times\sqrt{3}$-Ag) structure is formed at approximately one ML and further deposition results in a nucleation of 3D Ag islands.[1] The formation of $\sqrt{3}\times\sqrt{3}$-Ag has been reported to proceed with the creation of hole-island pairs of the $\sqrt{3}\times\sqrt{3}$-Ag structure.[10–12] The restructuring to $\sqrt{3}\times\sqrt{3}$-Ag at 240 °C was observed when the Ag island was larger than four times the size of a half of the 7×7 unit cell,[10,11] which was explained by the existence of a critical size of Ag islands on 7×7. To our knowledge, there are still few detailed studies on the critical size of Ag islands in the transformation from 7×7 to $\sqrt{3}\times\sqrt{3}$-Ag.

Second-harmonic generation (SHG), which is a technique capable of *in situ* measurement and is sensitive to the symmetry of surface structures, has already been successfully applied to the study of 7×7. The 7×7 structure is known to generate a strong SH signal at 1.17 eV, the fundamental frequency of the yttrium aluminum garnet (YAG) laser, which has been attributed to the resonance enhancement due to the surface-state transitions.[13–15] By Ag deposition onto 7×7 at RT, the SH intensity decays monotonically down to zero at a Ag coverage of about 1 ML.[16] The decay in the SH intensity signifies the quenching of the surface dangling bonds by the Ag adatoms.[16] In contrast, for Ag deposition at elevated temperatures above T_c, the SH intensity decreased until a Ag coverage of about 1/3 ML, and then increased for further Ag deposition until 1 ML, where the $\sqrt{3}\times\sqrt{3}$-Ag surfaces were formed.[17,18]

During our *in situ* monitoring of the change of the SH intensity induced by Ag deposition[17,18] above T_c, the initial delay was recognized to change with sample temperature; delay increased for lower temperatures approaching T_c. It was suggested that the delay might be related to the nucleation process of $\sqrt{3}\times\sqrt{3}$-Ag. Thus systematic experiments have been carried out to reveal the nucleation process.

In this paper, we report a series of *in situ* SHG measurements for Ag deposition onto the 7×7 surface at different substrate temperatures from 192 °C to 575 °C. We also measured the relative phases of the SH signals from 7×7 and $\sqrt{3}\times\sqrt{3}$-Ag at several temperatures. The desorption rates were obtained from *in situ* SHG results. The measured phase difference and the obtained desorption rates were successfully used to simulate the change of SH intensity during Ag deposition.

II. EXPERIMENTAL

The Si(111) wafer, with the size of $25\times4\times0.35$ mm^3, was placed in a UHV chamber with the longer side horizontal and along the $[2\bar{1}\bar{1}]$ direction. The pump for the SHG was 1064 nm (1.17 eV) radiation from a YAG laser, with a
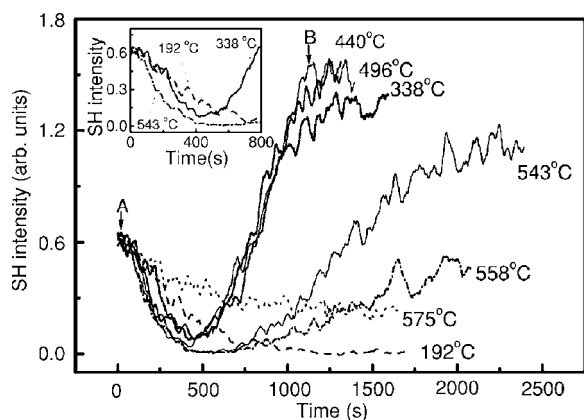
FIG. 1. The change of SH intensity during Ag deposition onto Si(111)-7×7 at various sample temperatures from 192 °C to 575 °C. The inset shows the plot of SH intensity from 0 to 800 s for three typical temperatures. The Ag flux was approximately 0.06 ML/min.

repetition rate of 10 Hz. For *in situ* observation, the laser was obliquely incident at an angle of 45° and focused to a spot with a diameter of 2 mm on the sample. The SH signal was detected along the reflected direction by a photomultiplier tube through a monochromator tuned at 532 nm. The input beam was vertically polarized along the $[01\bar{1}]$ direction of the sample. The SH signal was detected in the polarization direction perpendicular to the input polarization. The sample was flashed at a temperature of 1150 °C to expose a clean 7×7 surface by resistive heating of the sample through a direct current source. The sample temperatures above 400 °C were measured using an optical pyrometer with a nominal accuracy specified by the manufacturer of ±4 °C for temperatures lower than 800 °C. Due to a limited accuracy of the Si emissivity used in our experiment, the accuracy of the temperature measurement would be around ±10 °C. Temperatures lower than 400 °C were estimated using the temperature to current relationship developed by Ichikawa and Ino,[19] i.e., $\ln T = A \ln I + B$. This estimation procedure would allow an error of ±20 °C. Silver flux from a Knudsen-Cell (Kcell) was incident almost normally onto the sample. The UHV chamber was capable of an ultimate vacuum better than 2×10^{-10} Torr. The pressure in the chamber was below 5×10^{-10} Torr at all times during the experiment. The sample temperature was kept constant during Ag deposition. The relative phase of the SH signal was measured from the interference between SH signal from the sample with that from a *y*-cut quartz plate mounted on a translation stage in the output line in air.[20]

III. RESULTS AND DISCUSSION

The change of the $S_{in}P_{out}$ signal during Ag deposition onto a clean 7×7 surface is shown in Fig. 1 for various sample temperatures, where the SH intensity from a clean 7×7 surface is normalized to a constant value. The SH intensity decreased monotonically at 192 °C. As reported in the literature,[1] the phase transformation to $\sqrt{3} \times \sqrt{3}$-Ag does

not occur when the temperature is lower than T_c. At temperatures above T_c, an accelerated decrease of the SH intensity occurred, particularly up to the Ag coverage of about 1/3 ML; this is related to the phase transformation to $\sqrt{3} \times \sqrt{3}$-Ag. Moreover, a careful investigation of the initial stage of the decrease revealed that, at 338 °C, the decrease of the SH intensity showed a delay until around 200 s, compared with that at the highest temperature. A delay until around 80 s was also identified at 440 °C. For still higher temperatures in Fig. 1, the decreases of SH intensities were sufficiently rapid to make the delay less discernible. Almost no difference was observed in the increase of the SH intensity in the temperature range between 338 °C and 496 °C, as can be seen in Fig. 1. The increase was clearly much slower at 543 °C, which was found to be due to the slow increase of Ag coverage caused by Ag desorption, as will be discussed below. The SH signals in the initial stage of Ag deposition at three typical temperatures are shown in the inset of Fig. 1. The decrease at 338 °C was similar to that at 192 °C up to 200 s, but deviated with further Ag deposition. At 543 °C, the deviation began much earlier, from at least about 100 s.

The delay of the decrease of the SH intensity at 338 °C, as shown in Fig. 1, may be related to the nucleation of $\sqrt{3} \times \sqrt{3}$-Ag. For the nucleation of a new structure, the nucleus size must exceed a critical size to grow larger.[21] Since the transformation to $\sqrt{3} \times \sqrt{3}$-Ag is an activated process, Ag islands must also grow to a certain size to surmount the energy barrier before they can transform into $\sqrt{3} \times \sqrt{3}$-Ag. In the following discussion, in order to evaluate the delay of the phase transformation, we will express the SH intensity as a function of the Ag coverage and sample temperature, and then compare the experimental data shown in Fig. 1 with the temporal dependence of the SH intensity simulated according to the "direct transformation model," in which all the Ag atoms of less than 1 ML are assumed to instantaneously transform into $\sqrt{3} \times \sqrt{3}$-Ag.

The Si(111) surface is known to be a mixture of 7×7 and $\sqrt{3} \times \sqrt{3}$-Ag for a small amount of Ag deposition at sample temperatures higher than but close to T_c.[7] At higher sample temperatures of around 600 °C, Si(111)-3×1-Ag (hereafter referred to as 3×1-Ag) may coexist on the surface.[7,22,23] Then the SH intensity for Ag coverages less than 1 ML can be expressed as the sum of each contribution

$$I_{SHG} \propto \left\| \chi_1 \right| S_1 e^{i\varphi_1} + |\chi_2| S_2 e^{i\varphi_2} + |\chi_3| S_3 e^{i\varphi_3} |^2, \quad (1)$$

where χ, S, and φ are the second-order nonlinear susceptibility and the area and the phase of the SH response, respectively. The subscripts 1, 2, and 3 represent 7×7, $\sqrt{3} \times \sqrt{3}$-Ag, and 3×1-Ag, respectively. The intensity of the observed SH signal is a superposition of all the SH responses from coexisting structures.

First, let us estimate the SH contribution from the 3×1-Ag structure. In Fig. 2, the change of the $S_{in}S_{out}$ signal during Ag deposition onto the 7×7 surface is plotted as a function of time. No $S_{in}S_{out}$ signal, except for the dark count of the photomultiplier tube (PMT), was observed for either the 7×7 or the $\sqrt{3} \times \sqrt{3}$-Ag structure,[16,17] as expected from their 3m symmetry. Thus the $S_{in}S_{out}$ signal can originate only from 3×1-Ag or its related structures.[17] Although the details
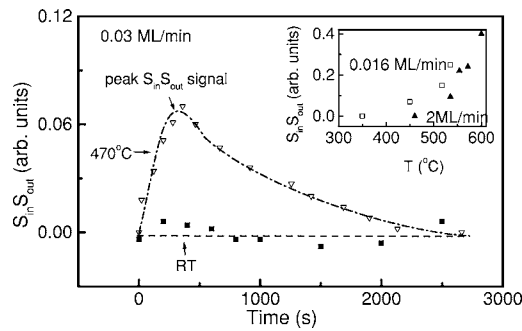
FIG. 2. The change of $S_{in}S_{out}$ signal from Si(111)-3×1-Ag during Ag deposition onto Si(111)-7×7 at RT and 470 °C. The Ag flux was 0.03 ML/min. The inset shows the sample temperature dependence of the peak $S_{in}S_{out}$ signal observed during Ag deposition onto Si(111)-7×7. The Ag fluxes were approximately 0.016 and 2 ML/min, respectively.

of the origin of the $S_{in}S_{out}$ signal are still unclear, the $S_{in}S_{out}$ signal intensity can be assumed to be proportional to the square of the 3×1-Ag area.[17] As shown in Fig. 2, the peak $S_{in}S_{out}$ signal intensity observed during Ag deposition at 470 °C was about 1/9 of that observed during Ag desorption, which we consider to correspond to a nearly full 3×1-Ag surface.[17] No signals from 3×1-Ag were recognized for temperatures lower than 400 °C. Moreover, the SH signal from 3×1-Ag was much weaker during adsorption than during desorption. Thus, we simply assume that the contribution to $S_{in}P_{out}$ from 3×1-Ag can be neglected in Fig. 1, particularly for low Ag coverage at temperatures lower than 450 °C.

We will consider only the contributions from 7×7 and $\sqrt{3}\times\sqrt{3}$-Ag. Then the expression for the SH intensity can be simplified to

$$I_{SHG} \propto \left| |\chi_1|S_1 e^{i\varphi_1} + |\chi_2|S_2 e^{i\varphi_2} \right|^2$$
$$= |\chi_1|^2 S_1^2 + |\chi_2|^2 S_2^2 + 2|\chi_1|S_1|\chi_2|S_2 \cos(\varphi_1 - \varphi_2). \quad (2)$$

Then, χ, S, and $\varphi_1-\varphi_2$ can be evaluated from experimental data as follows. The ratio of the nonlinear susceptibility of $\sqrt{3}\times\sqrt{3}$-Ag to that of 7×7, $|\chi_2/\chi_1|$ was obtained from the ratio of the signals at B and A in Fig. 1 since B corresponds to a full $\sqrt{3}\times\sqrt{3}$-Ag surface. In the simulation, we used the same ratio at all sample temperatures since little difference was observed in the ratios.

Figure 3 shows the typical phase measurement results at RT and 460 °C. By fitting the experimental data using the sine function, we obtained 148° and 155° for the phase differences between 7×7 and $\sqrt{3}\times\sqrt{3}$-Ag at RT and 460 °C, respectively. Then the change of the SH intensity with Ag deposition above T_c can clearly be interpreted by the destructive interference resulting from the phase difference of 150°. We assume that the phase difference is temperature independent and is 150° at all the employed temperatures, although we note that the absolute phase of the SH signal from 7×7 was slightly dependent on temperature.[20] Note that even if we include the slight temperature dependence of the phase difference, the following conclusions will be little affected.
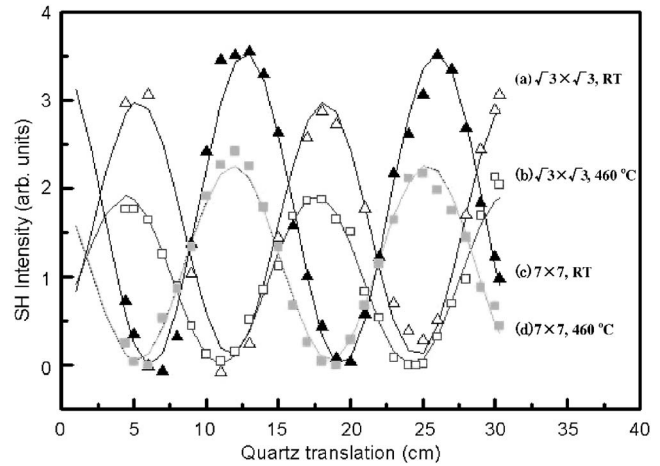
FIG. 3. Interference pattern of the SH signal as a function of the distance that a quartz reference moved from its original position for (a) Si(111)-$\sqrt{3}\times\sqrt{3}$-Ag at RT, (b) Si(111)-$\sqrt{3}\times\sqrt{3}$-Ag at 460 °C, (c) Si(111)-7×7 at RT, and (d) Si(111)-7×7 at 460 °C. The symbols represent the experimental data and the solid lines are the fitted results.

Next, we will evaluate the temperature dependence of the contribution of desorption to S_1 and S_2. S_1 and S_2 can be expressed by θ. Because the Ag coverage of $\sqrt{3}\times\sqrt{3}$-Ag surface is 1 ML, the area of $\sqrt{3}\times\sqrt{3}$-Ag (S_2) can be expressed by θ in our simple model, while the area of 7×7 (S_1) is $1-\theta$, where $\theta(t)$ can be described by the rate equation $d\theta/dt = A - D\theta$ with A being the Ag flux and D the desorption rate. The sticking probability of Ag atoms is taken to be 1 for Ag coverages less than 1 ML.[24] Using the solution of the rate equation, $\theta = A/D(1-e^{-Dt})$, the areas of 7×7 and $\sqrt{3}\times\sqrt{3}$-Ag can then be expressed by $S_1 = 1-\theta = 1-A/D(1-e^{-Dt})$ and $S_2 = \theta = A/D(1-e^{-Dt})$, respectively. The desorption rate D was obtained from the isothermal experimental results, as shown in the inset of Fig. 4, where the initial 7×7 surface had no $S_{in}S_{out}$ signal. During Ag deposition, the $S_{in}S_{out}$ signal increased in response to the growth of 3×1-Ag, and then, after a peak, it decreased gradually to
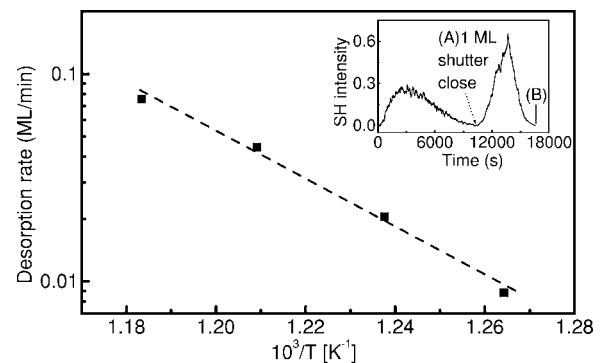
FIG. 4. Desorption rates of Ag atoms from Si(111)-$\sqrt{3}\times\sqrt{3}$-Ag versus the sample temperature (Arrhenius plots). The inset shows the results of an *in situ* SH measurement used for the estimation of desorption rate at a sample temperature of 543 °C, where (A) corresponds to a Si(111)-$\sqrt{3}\times\sqrt{3}$-Ag surface and (B) corresponds to a Si(111)-7×7 surface.
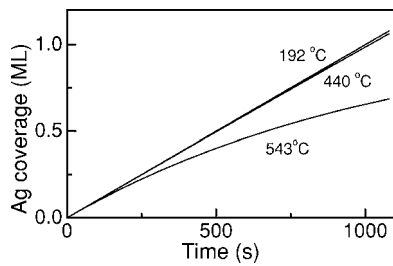
FIG. 5. Deposition time dependence of Ag coverage θ calculated from the desorption rates shown in Fig. 4.

FIG. 6. Simulation and experimental results for several typical sample temperatures. Dotted lines are the simulation results and solid lines are the experimental results. The experimental results have been normalized to 1 for the signal from clean 7×7.

zero at 1 ML. After closing the shutter at A (see the inset), the $S_{in}S_{out}$ signal again started to increase in response to Ag desorption. The peak $S_{in}S_{out}$ signal corresponding to the largest 3×1-Ag area appeared during Ag desorption. At the end of desorption, indicated by B, the $S_{in}S_{out}$ signal was again zero, corresponding to a surface fully covered by 7×7. Since the desorption energies reported for $\sqrt{3} \times \sqrt{3}$-Ag and 3×1-Ag are sufficiently close, 64 and 69 kcal/mol, respectively,[24] it may be reasonable to use the same rate for Ag desorption from $\sqrt{3} \times \sqrt{3}$-Ag and 3×1-Ag. The Ag coverage can then be expressed by $\theta = e^{-Dt}$, according to a simple rate equation, by taking $t=0$ at A, where D and θ represent the desorption rate and Ag coverage, respectively. If we assume that the peak $S_{in}S_{out}$ signal observed during Ag desorption from $\sqrt{3} \times \sqrt{3}$-Ag corresponds to Ag coverage of 1/3 ML, we can numerically evaluate D. Figure 4 shows the Arrhenius plot of D versus $1/T$, where T is the sample temperature in Kelvin. A desorption energy of 59 kcal/mol was obtained from Fig. 4, which is sufficiently close to the reported value of 64 and 69 kcal/mol for $\sqrt{3} \times \sqrt{3}$-Ag and 3×1-Ag, respectively. This may, in turn, confirm our interpretation that the $S_{in}S_{out}$ signals come from 3×1-Ag and the peak $S_{in}S_{out}$ signals observed during Ag desorption correspond to a surface fully covered by 3×1-Ag with a Ag coverage of 1/3 ML.[17]

Figure 5 shows the calculated Ag coverage for 192 °C, 440 °C, and 543 °C. The increase of Ag coverage at 543 °C or higher is clearly slower than those at 338 °C or 440 °C, as a result of stronger Ag desorption. This clearly indicates a negligible contribution of desorption at sample temperatures up to 440 °C.

The time dependences of the SH intensities shown by the dotted lines in Figs. 6(b), 6(c), and 6(d) are thus calculated from Eq. (2) using S_1 and S_2 obtained from the desorption rates. The experimental results normalized by 1 for the SH intensity from a 7×7 surface are also plotted as solid lines for comparison. The decrease of the SH intensity in Fig. 6(a) can be attributed to the quenching of the surface states of 7×7,[16] because the sample temperature of 192 °C was not high enough for the phase transformation to $\sqrt{3} \times \sqrt{3}$-Ag to occur. Thus the SH intensity at 192 °C may be expressed by $I \propto (1-\theta)^2$ if we assume that the 7×7 area is quenched in proportion to the Ag coverage θ up to 1 ML. This assumption may be justified by the change of the SH intensity being well reproduced using this expression, as shown by the solid line in Fig. 6(a). For the case of 338 °C shown in Fig. 6(b), there exists a large discrepancy between the experimental
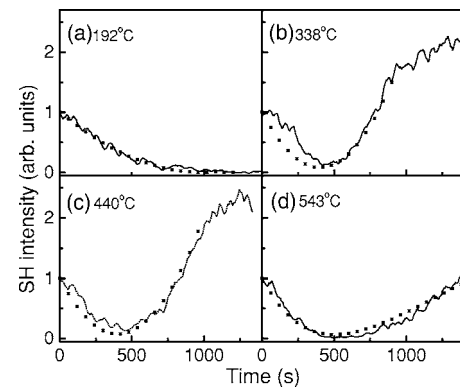
data and the simulation before 500 s, while the simulation agrees better with the experimental data after 500 s. At 440 °C, the discrepancy before 500 s is clearly smaller than that at 338 °C. In Fig. 6(d), where the sample temperature was 543 °C, the discrepancy before 500 s is much smaller.

The rapid decrease of the simulation data reflects the cancellation of the signals from 7×7 and $\sqrt{3} \times \sqrt{3}$-Ag because their phase difference of around 150° results in a destructive interference as has been discussed above. Since there were no structures other than 7×7 and $\sqrt{3} \times \sqrt{3}$-Ag existing on the surface at the temperature of 338 °C, the slower decrease of the experimental data compared to the results of the simulation based on the direct transformation model can be attributed only to a delay of the phase transformation, i.e., a smaller area of $\sqrt{3} \times \sqrt{3}$-Ag in the initial stage of Ag deposition compared to that determined by the model. Figure 6(c) shows a similar behavior at 440 °C, but with a smaller discrepancy between the simulation and experimental results. A possible small contribution from 3×1-Ag was neglected in the case of Figs. 6(c) and 6(d). Even if we change $\varphi_1 - \varphi_2$ by 10°, the simulation results show negligible deviation from the results in Figs. 6(b) and 6(c). This will justify our assumption of a temperature-independent $\varphi_1 - \varphi_2$.

Thus, Fig. 6 indicates that the phase transformation from 7×7 to $\sqrt{3} \times \sqrt{3}$-Ag does not occur instantaneously following Ag deposition. The delay in the initial stage of Ag deposition is shown to decrease with increasing temperature. After the delay, the transformation appears to be accelerated to catch up with the transformation in proportion to the Ag coverage. The delay of the decrease of the SH intensity shown in Fig. 1 may correspond to the transformation being able to start only after the Ag island reaches a critical size. Once the $\sqrt{3} \times \sqrt{3}$-Ag nuclei are formed, the transformation will be accelerated because of the low barrier energy for growth, until all of the deposited Ag atoms are incorporated into the $\sqrt{3} \times \sqrt{3}$-Ag transformation. Considering the low barrier energy for the transformation at high temperatures, the shorter delay at high temperatures shown in Fig. 1 may be explained either by a smaller critical cluster size at high temperatures or a faster diffusion of Ag atoms at high temperatures. A detailed quantitative study of the nucleation and growth process is now under way.

IV. CONCLUSION

A delay of the decrease of SH intensity was observed during Ag deposition onto a 7×7 surface at elevated sample temperatures. The temporal dependence of the SH intensity calculated for the case of direct transformation to Si(111)-$\sqrt{3} \times \sqrt{3}$-Ag shows a temperature-dependent deviation from the experimental data. These results suggest that a critical nucleus for the growth of Si(111)-$\sqrt{3} \times \sqrt{3}$-Ag can be identified. The peak of a polarization-selected SHG signal observed during desorption was also found to correspond to a surface fully covered by 3×1 structure with a Ag coverage of 1/3 ML.

---

*Corresponding author. Electronic address: tsuzuki@riken.jp

[1] S. Hasegawa, X. Tong, S. Takeda, N. Sato, and T. Nagao, Prog. Surf. Sci. **60**, 89 (1999).

[2] T. Jarolĺmek, J. Mysliveček, P. Sobotĺc, and I. Ošt'ádal, Surf. Sci. **482-485**, 386 (2001).

[3] G. Lelay, M. Manneville, and R. Kern, Surf. Sci. **72**, 405 (1978).

[4] W. C. Fan and A. Ignatiev, Phys. Rev. B **41**, 3592 (1990).

[5] S. Kohmoto and A. Ichimiya, Appl. Surf. Sci. **33/34**, 45 (1988).

[6] G. Raynerd, M. Hardiman, and J. A. Venables, Phys. Rev. B **44**, 13803 (1991).

[7] A. W. Denier van der Gon and R. M. Tromp, Phys. Rev. Lett. **69**, 3519 (1992).

[8] N. Sato, T. Nagao, S. Takeda, and S. Hasegawa, Phys. Rev. B **59**, 2035 (1999).

[9] G. Lelay, Surf. Sci. **132**, 169 (1983), and references listed therein.

[10] A. Shibata, Y. Kimura, and K. Takayanagi, J. Vac. Sci. Technol. B **12**, 2026 (1994).

[11] A. Shibata, Y. Kimura, and K. Takayanagi, Surf. Sci. **303**, 161 (1994).

[12] D. W. McComb, D. J. Moffatt, P. A. Hackett, B. R. Williams, and B. F. Mason, Phys. Rev. B **49**, 17139 (1994).

[13] U. Höfer, Appl. Phys. A **63**, 533 (1996).

[14] K. Pedersen and P. Morgen, Surf. Sci. **377-379**, 393 (1997).

[15] T. Suzuki, Phys. Rev. B **61**, R5117 (2000).

[16] R. Venkataraghavan, M. Aono, and T. Suzuki, Surf. Sci. **517**, 65 (2002).

[17] D. Deng and T. Suzuki, Jpn. J. Appl. Phys., Part 2 **43**, L510 (2004).

[18] D. Deng, M. Numata, and T. Suzuki, J. Phys. Soc. Jpn. **73**, 3384 (2004).

[19] T. Ichikawa and S. Ino, Surf. Sci. **105**, 395 (1981).

[20] T. Suzuki, D. E. Milovzorov, S. Kogo, M. Tsukakoshi, and M. Aono, Appl. Phys. B **68**, 623 (1999).

[21] M. Ohring, *The Materials Science of Thin Films* (Academic Press, San Diego, 1992), p. 41.

[22] K. J. Wan, X. F. Lin, and J. Nogami, Phys. Rev. B **47**, 13700 (1993).

[23] K. Sakamoto, H. Ashima, H. M. Zhang, and R. I. G. Uhrberg, Phys. Rev. B **65**, 045305 (2001).

[24] S. Hasegawa, H. Daimon, and S. Ino, Surf. Sci. **186**, 138 (1987).